Field-to-Wire Coupling Model for the Common Mode in Random Bundles of Twisted-Wire Pairs

Giordano Spadacini, *Member, IEEE*, Flavia Grassi, *Senior Member, IEEE*, and Sergio A. Pignari, *Fellow, IEEE*

I. Introduction

RANDOM bundles of wires obtained by hand-made assembly are widely used in large electrical/electronic systems (e.g., in the aerospace and automotive sectors). Their electromagnetic modeling still represents a challenging problem as concerns prediction of crosstalk and field-to-wire coupling. Indeed, deterministic modeling based on the representation of specific and arbitrary cable geometries would be an exercise in futility, due to the high sensitivity of the induced noise to different random configurations of the bundle. Consequently, statistical models are more suited, since they are based on the description of model parameters and results in terms of random variables and their moments (e.g., mean, standard deviation, etc.) [1]–[3]. Though the complexity of the involved electromagnetic problem prevents analytical closed-form solutions, the numerical Monte Carlo method (that is, repeated-run simulations carried out on several random samples of the bundle) is a common viable approach. Particularly, repeated-run analysis requires two fundamental tools: 1) a method to generate a physically sound geometry of random-bundle samples; 2) a fast solution method, so to optimize the computational burden associated with several simulations [4]. These aspects are here treated with a specific focus on the radiated susceptibility of random bundles composed of twisted-wire pairs (TWPs).

Recent papers proposed models of crosstalk [5], [6] and field coupling [7]–[10] for a single TWP or a TWP bundle. Among these, field coupling to a bundle composed of parallel TWPs above ground (i.e., having deterministic position of their axes in the bundle cross-section) was analyzed in [9], where the concepts of averaged per-unit-length (p.u.l.) parameters and balanced interconnection were exploited to represent the nonuniform wiring structure as a uniform multiconductor transmission line (MTL). Additionally, pure common-mode (CM) excitation of each TWP in the bundle was considered as the dominant radiated-susceptibility effect (i.e., small differences in the incident field sensed by each wire in a pair were neglected, thanks to ideal symmetry ensuing from twisting). As a consequence, model input in [9] was an incident electric-field approximated by a discrete set of samples along the bundle path (which may be the output of any full-wave electromagnetic solver), and model outputs were the frequency responses of 1) CM noise induced at terminal loads of each TWP, and 2) that part of differential-mode (DM) noise arising from CM-to-DM conversion due to termination unbalance.

In [9], reported observations about the significant difference between CM noise responses pertaining to different TWPs (notwithstanding equal wires and terminal loads), depending on their position in the bundle cross-section, is a fundamental motivation for this study. Namely, it follows that the approach in [9] may be unreliable for bundles characterized by uncontrolled geometry.

This study extends the approach proposed in [9] to bundles composed of TWPs whose positions along the cable path are subject to random changes. Section II defines the structure geometry, based on a deterministic reference cross-section. From this, many different cross sections can be randomly generated by swapping TWP positions as explained in Section III. The field-to-wire coupling model is presented in Section IV and validated in Section V. Finally, Section VI exemplifies the statistical analysis of the induced noise for a random TWP bundle under plane-wave excitation, and Section VII draws concluding remarks.

Manuscript received September 11, 2014; revised December 22, 2014; accepted February 17, 2015. Date of publication April 1, 2015; date of current version October 12, 2015.

The authors are with the Department of Electronics, Information and Bioengineering, Politecnico di Milano 20133, Milano Italy (e-mail: giordano.spadacini@ polimi.it; flavia.grassi@ polimi.it; sergio.pignari@ polimi.it).

Color versions of one or more of the figures in this paper are available online.

II. Random Bundle of Twisted-Wire Pairs

A. Geometry of the Structure Under Analysis

The structure under analysis is a hand-made bundle composed of TWPs running above a metallic ground. As sketched in Fig. 1(a), paths of TWPs are random and uncontrolled along the bundle length. Namely, the path of each TWP can be concerned

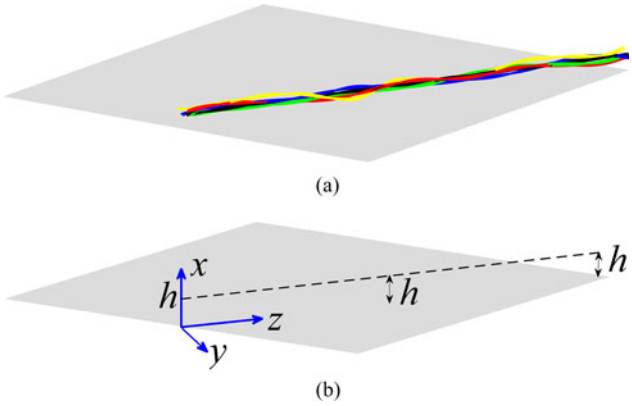

Fig. 1. In the considered bundle: (a) TWPs follow random paths along the bundle, but (b) the path of the bundle axis (dashed line with constant height *h* above ground) is deterministic.

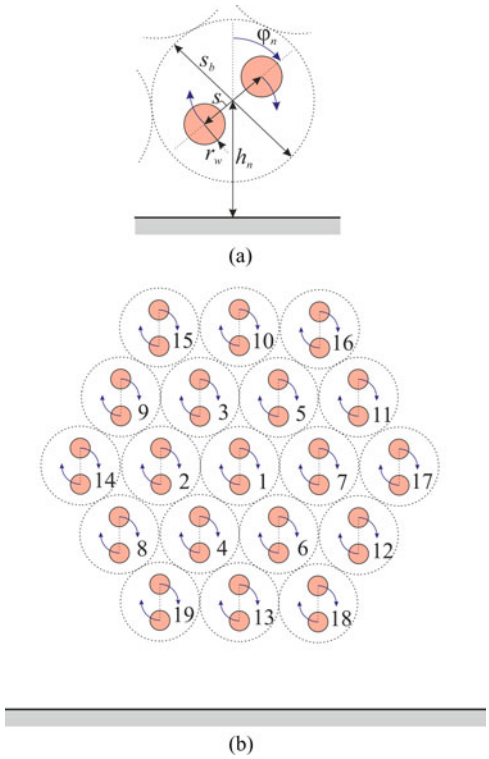

Fig. 2. Cross-sections of the structure under analysis: (a) Definition of geometrical parameters of each TWP. (b) Reference cross-section composed of $N = 19$ TWPs. Each dotted circle in (b) has the structure shown in (a).

as a random displacement from an expected value, represented by the path of the bundle axis, which is assumed to be deterministic, i.e., a known curve in a local Cartesian reference system (x, y, z). As an additional assumption, the height h above ground of such a bundle axis is the same over the whole bundle length, as shown in Fig. 1(b).

The two wires forming each TWP are wound into a bifilar helix along their length, as shown in the principle drawing of Fig. 2(a), where the cross section of a TWP is sketched as a rotating wire-pair enclosed in a circular region (dashed black circle). The involved geometrical parameters are the wire radius r_w, wire separation s, and pair separation in the bundle s_b, which are common to all TWPs in the bundle. Conversely, h_n denotes the height above ground of the nth TWP. In practical cables, the separations s and s_b are determined, to a large extent, by the thickness of the dielectric insulation surrounding each wire. However, wires in free space are considered here, since the impact of such a simplification was investigated in [9, Section IV-C] and found to be acceptable for practical purposes (errors limited to a few dBs in the amplitude of the induced CM noise, and possible slight shift of resonance frequencies).

B. Reference Cross-Section

The proposed prediction model is based on the definition of a reference cross-section, whose axis is placed at a constant height h above ground, intended as the mean of TWP heights h_n. TWPs are tightly packed and arranged in pseudocircular form. If N is the number of TWPs, the number of wires is $2\times N$, and the total number of conductors, including ground, is $2 \times N + 1$.

Without loss of generality, a valid pseudocircular cross-section with $N = 19$ is defined in Fig. 2(b). The generality of this choice stems from the possibility—by virtue of the proposed TWP numbering—to arbitrarily reduce the number of TWPs, while preserving the compactness of the structure. In other words, if a bundle with $2 \leq N \leq 19$ has to be analyzed, TWPs with labels exceeding N will be removed from Fig. 2(b), while the resulting cross section will retain a valid, compact structure. Otherwise, the approach can be easily extended for $N > 19$.

The introduction of a reference cross-section is aimed at speeding up the solution process. Indeed, p.u.l. parameters (inductances, capacitances) randomly fluctuate along a nonuniform bundle; therefore, they should be evaluated for several different cross-section configurations. However, a reference cross-section can be used to evaluate a reference set of p.u.l. parameters only once and to obtain several different sets, all consistent with the original pseudocircular structure, through suitable matrix permutations. It is worth noting that Fig. 2(b) is not the only possible definition for a tightly packed cross-section [2], [4], [11]. However, it has been verified that, as long as a *statistical* analysis (i.e., aimed at predicting a statistical population of results, and their estimates) of *random* bundles is the target, this specific choice has a minor impact on results [11].

III. Randomization of the Cross Section

The bundle can be modeled as a *nonuniform* MTL which is approximated by cascading *uniform* MTL sections, each one having constant p.u.l. parameters [12]. It is worth noting that nonuniformity stems from a twofold reason. First, each TWP is composed of two rotating wires. Second, TWP positions are randomly variable along the bundle path. Correspondingly, two heuristic assumptions are involved in the proposed approximation:

1) A TWP whose axis is invariable (i.e., constant height) behaves as a balanced differential pair characterized by constant p.u.l. parameters averaged over a twisting period

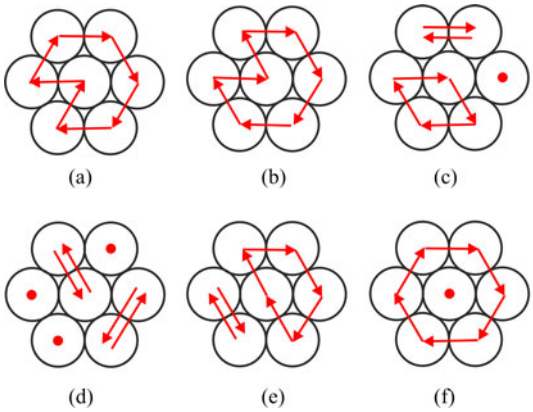

Fig. 3. Six examples of cycles for a reference cross-section with $N = 7$ TWPs. Two Hamiltonian cycles are shown in (a) and (b).

[13]. As shown in [7] and [9] and recalled in Section IV-A, this approach eliminates nonuniformity associated to wire twisting.

2) There exists a characteristic bundle length $\mathscr{L}_c$. along which the relative position of each TWP axis in the cross section is approximately invariable. More exactly, TWP axes either stay in their positions or move *at most* to a distance s_b. Such a characteristic dimension is associated with peculiarities of cable construction, that is, to the smoothness of TWP paths resulting from the assembly method. In the author's experience, this parameter can be easily estimated (it does not require exact determination) by inspection of bundle samples.

Accordingly, the TWP bundle can be subdivided into N_S equal uniform sections having lengths $\mathscr{L} \approx \mathscr{L}_c$. It is worth stressing that this section length is uncorrelated with the wavelength (it is only related to the geometrical features of the random cable). Therefore, bundle subdivision into N_S sections does not involve any frequency limitation to model validity.

Between two subsequent bundle sections, TWP movements occur at most between adjacent positions. Specifically, one can assume that all cross sections are similar and obtained by allowing minimum-distance interchanges of TWPs in the reference cross-section of Fig. 2(b). The set of such position interchanges is called *cycle*. As an illustrative example, six cycles for $N = 7$ TWPs are shown in Fig. 3. Arrows represent shifts between adjacent positions, whereas dots denote TWPs which do not move.

The determination of all possible cycles is a so-called "NP complete" problem in the framework of Graph Theory [14]. Namely, one can define a graph whose nodes are TWP positions and whose branches connect adjacent nodes (i.e., adjacent TWP positions in the reference cross-section). The solution consists in finding all possible routes in the graph, including the possibility to exclude from a route the positions occupied by those TWPs which do not move [see Fig. 3(f)], and including disjoint routes [see Fig. 3(e)]. A special case is represented by the so-called Hamiltonian cycles, i.e., single routes between all nodes [see Fig. 3(a) and (b)]. This mathematical problem

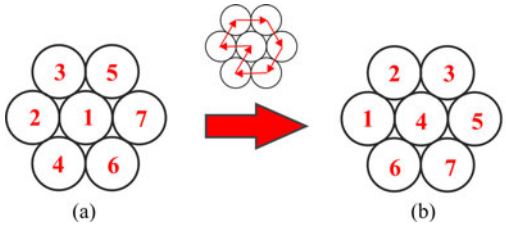

Fig. 4. Example of application of a cycle.

TABLE I
NUMBER OF POSSIBLE CYCLES—CROSS-SECTION IN FIG. 2(B)

Number of TWPs	Number of possible cycles
$N = 2$	2
$N = 3$	6
$N = 4$	14
$N = 5$	31
$N = 6$	64
$N = 7$	212
$N = 8$	456
$N = 9$	893
$N = 10$	1769
$N = 11$	3448
$N = 12$	6933
$N = 13$	12 363
$N = 14$	45 567
$N = 15$	152 075
$N = 16$	502 499
$N = 17$	1 661 436
$N = 18$	5 439 076
$N = 19$	16 043 600

can be very time consuming. However, for a given reference cross-section and a given number N of TWPs, it must be solved once and for all and the obtained results can be conveniently stored. To optimize memory occupation, a cycle is concisely represented by an array $\boldsymbol{c}$ having elements $c_n, n = 1, 2, \ldots, N$ such that the integer c_n is the TWP number (univocally defined in the reference cross-section) moving to position n. For instance, $c = [4, 1, 2, 6, 3, 7, 5]$ describes the Hamiltonian cycle in Fig. 3(a) which is applied to the reference cross-section in Fig. 4(a) to yield the cross section in Fig. 4(b). The number of possible cycles rapidly increases with N, according to the larger number of bundle configurations enabled by a larger number of pairs. Specifically, for the reference cross-section in Fig. 2(b), all possible cycles have been identified and their total number is reported in Table I.

Once the population of all possible cycles is available, a sample of TWP bundle can be constructed by randomly selecting a set of N_S cycles according to a uniform-discrete probability distribution. Each cycle is applied to a bundle section to obtain the arrangement of TWPs for the subsequent bundle section (the first cycle being applied to the reference cross-section). By this approach, one can construct several samples of random bundles. Four examples are shown in Fig. 5, for a bundle composed of $N = 7$ TWPs, and $N_S = 10$ sections with equal length $\mathscr{L} = 10$ cm. The same color represents the same TWP in the bundle. To preserve figure readability, only five out of the seven TWPs are

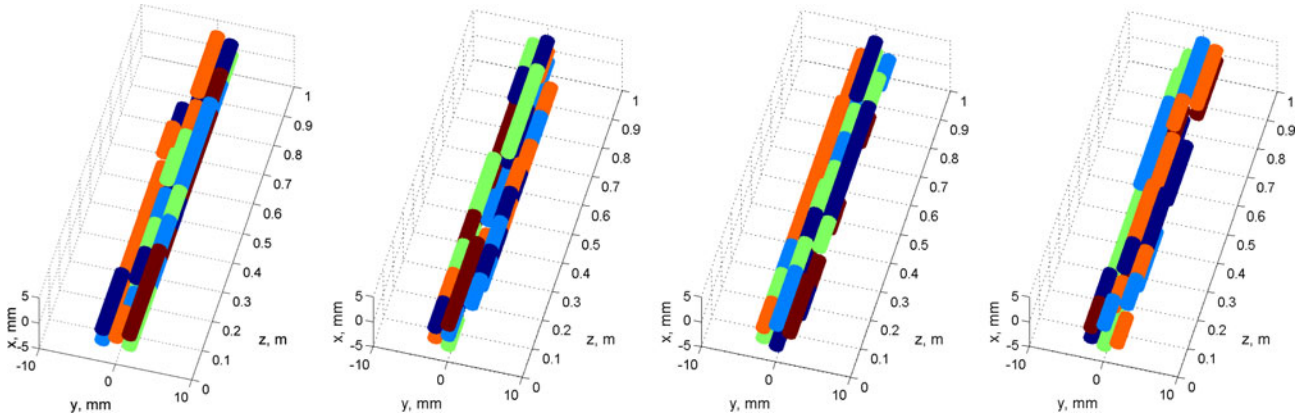

Fig. 5. Simplified sketch of four samples of a random bundle ($N_S = 10$ bundle sections, $N = 7$ TWPs). For graphical readability, only five of the seven TWPs are represented with colored tubes, and Cartesian axes have different scales.

actually represented (by tubular cylinders), and the transversal dimensions are magnified with respect to the longitudinal dimension. It can be appreciated that the proposed method allows the approximation of random bundles with smooth and physically sound transitions in the cross section, since it assures that all TWP shifts occur between adjacent positions only.

IV. Field-to-Wire Coupling Model

Given that all possible cross sections are obtained by interchanging TWP positions in the reference cross-section of Fig. 2(b), the MTL model can be computed only once. Indeed, MTL models pertaining to different bundle sections can be evaluated starting from this reference MTL model through simple permutations of conductors. Finally, the whole MTL model of the bundle is obtained from the cascade-connection of all bundle sections.

A. MTL Model for the Reference Bundle Section

The field-to-wire coupling model for a TWP bundle running above ground and having a defined cross section, that is, fixed and straight positions of TWP axis, was developed and validated in [9]. Here, the same approach is used to construct an MTL model for the *reference* bundle section having the cross section in Fig. 2(b). Main aspects are only briefly summarized here, whereas the reader is referred to [9] for more details and for a thorough discussion of validity limits.

The nonuniform MTL (where nonuniformity stems only from wires rotation in each TWP) is treated as an equivalent uniform MTL with constant, averaged, p.u.l. parameters. Rationale for this assumption is based on the ideal symmetry ensuing from wire twisting (indeed, the twist pitch is assumed to be much shorter than the section length), which allows treating the TWP bundle as a superbalanced structure, that is, a bundle composed of perfectly balanced pairs. Practical validity limits of this approach are $s \geq 4r_w$, $s_b \geq s + 4r_w$, $h_n \geq 3s, \forall n$, [9]. By virtue of this assumption, the $2N \times 2N$ p.u.l. inductance matrix $\boldsymbol{L}$ of the MTL can be partitioned in 2×2 submatrices as

$$\boldsymbol{L} = \begin{bmatrix} \bar{\boldsymbol{L}}_1 & \bar{\boldsymbol{M}}_{12} & \dots & \bar{\boldsymbol{M}}_{1N} \\ \bar{\boldsymbol{M}}_{12} & \bar{\boldsymbol{L}}_2 & \dots & \bar{\boldsymbol{M}}_{2N} \\ \dots & \dots & \dots & \dots \\ \bar{\boldsymbol{M}}_{1N} & \bar{\boldsymbol{M}}_{2N} & \dots & \bar{\boldsymbol{L}}_N \end{bmatrix}. \tag{1}$$

Each submatrix $\bar{\boldsymbol{L}}_n$, $n = 1, 2, \dots, N$, is a 2×2 symmetric matrix exhibiting two equal in-diagonal, $\bar{l}_n$, and off-diagonal, $\bar{l}_{M,n}$, entries that represent the averaged p.u.l. self- and mutual-inductances of the wires belonging to the *n*th pair, respectively. Additionally, each submatrix $\bar{\boldsymbol{M}}_{nk}$, *n,k* = 1, 2, …, *N,* is a 2×2 matrix containing four equal entries $\bar{l}_{n,k}$, representing averaged p.u.l. mutual inductances between wires belonging to the *n*th and *k*th TWP. The line placed above symbols is used to stress that the involved quantities represent averages over a twisting period. For instance, the self-inductance $\bar{l}_n$ is defined as

$$\bar{l}_n = \frac{1}{2\pi} \int_0^{2\pi} l_n(\varphi_n) d\varphi_n \tag{2}$$

where $l_n(\varphi_n)$ is the variable p.u.l. inductance depending on the tilt angle $\varphi_n \in [0, 2\pi]$ in Fig. 2(a), [8], [9]. Approximate closed-form expressions of averaged p.u.l. inductances can be obtained under particular assumptions [9], [15]. Finally, by recalling that any dielectric sheath is here neglected, the p.u.l. capacitance matrix of the MTL is computed by $\mathbf{C} = c_0^{-2}\mathbf{L}^{-1}$, where c_0 is the light speed in free-space [16].

The distributed-parameter circuit model is shown in Fig. 6(a). It is composed of a uniform MTL (passive part) represented by the chain-parameter matrix $\boldsymbol{\Phi}$, and two voltage sources (active part) at terminations. For a bundle with *N* TWPs, matrix $\boldsymbol{\Phi}$ has dimension 4*N*×4*N* with expression

$$\boldsymbol{\Phi} = \begin{bmatrix} \cos(\beta_0 \mathscr{L}) \mathbf{1}_{2N} & -j \boldsymbol{Z}_{\mathbf{C}} \sin(\beta_0 \mathscr{L}) \\ -j \boldsymbol{Z}_{\mathbf{C}}^{-1} \sin(\beta_0 \mathscr{L}) & \cos(\beta_0 \mathscr{L}) \mathbf{1}_{2N} \end{bmatrix} \tag{3}$$

where $\beta_0 = 2\pi f / c_0$ is the propagation constant, $\mathscr{L}$ is the length of the MTL section, $\mathbf{1}_{2N}$ denotes the 2*N*×2*N* unit matrix, and $\boldsymbol{Z}_{\mathbf{C}} = c_0 \boldsymbol{L}$ is the characteristic impedance matrix.

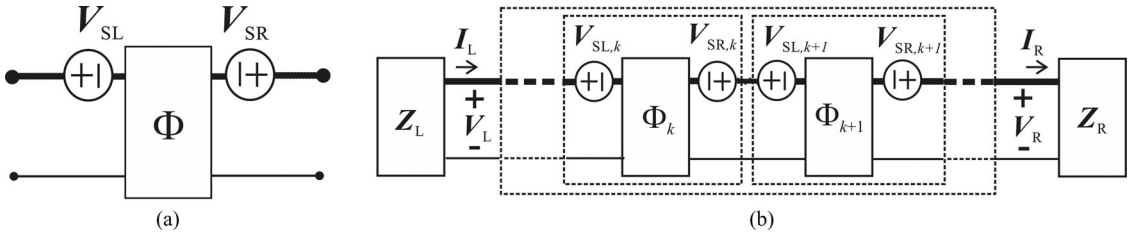

Fig. 6. MTL modeling of the TWP bundle: (a) Distributed-parameter circuit model of the reference section, and (b) circuit model for the computation of the terminal response (the thick line represents 2*N* wires, where *N* denotes the number of TWPs).

The voltage sources $\boldsymbol{V}_{\rm SL}$, $\boldsymbol{V}_{\rm SR}$ in Fig. 6(a) account for the CM noise induced by the external electromagnetic field in each TWP. Equal voltage sources act on the two wires of each pair, since wire rotation implies, on average, the cancellation of the DM noise component [9]. Therefore, $\boldsymbol{V}_{\rm SL}$, $\boldsymbol{V}_{\rm SR}$ are vectors with 2*N* entries given by

$$V_{{\rm SL},2n-1} = V_{{\rm SL},2n} = \int_0^{\mathscr{L}} \frac{\sin[\beta_0(z-\mathscr{L})]}{\sin(\beta_0\mathscr{L})} E_z(h_n,0,z)dz - \int_0^{h_n} E_x(x,0,0)dx \tag{4}$$

$$V_{{\rm SR},2n-1} = V_{{\rm SR},2n} = \int_0^{\mathscr{L}} \frac{\sin(\beta_0 z)}{\sin(\beta_0\mathscr{L})} E_z(h_n,0,z)dz - \int_0^{h_n} E_x\left(x,0\ ,\mathscr{L}\right)dx \tag{5}$$

where $n = 1, 2, \ldots, N$. According to the Agrawal model of field-to-wire coupling, (4)–(5) involve the superposition of two contributions: one due to the longitudinal component $E_z(x,y,z)$, and one due to the vertical component $E_x(x,y,z)$ of the incident electric field acting along the deterministic path of the bundle [17]–[19]. A numerical method for the approximation of (4)–(5) was developed in [9], where a discrete number of incident-field samples were considered as input data. For simple electromagnetic field structures (e.g., a uniform plane-wave), incident-field samples can be computed analytically, whereas for complex electromagnetic environments, these samples can be obtained by running any full-wave numerical solver [9].

B. MTL Models of Different Bundle Sections

Efficiency of the proposed approach stems from the fact that the MTL model in Section IV-A has to be evaluated only once for the reference cross-section in Fig. 2(b), and conveniently stored. Indeed, all other MTL models pertaining to the different $N_{\rm S}$ bundle sections can be obtained by permutations of rows and columns in vectors and matrices, according to the fact that application of a cycle involves swapping of TWPs.

To this end, a permutation matrix $\boldsymbol{P}$ with dimension $2N\times 2N$ can be associated with a cycle [11]. Namely, all entries of $\boldsymbol{P}$ are equal to zero, with the exception of

$$P_{2i-1,2j-1} = P_{2i,2j} = 1, \text{if TWP } i \text{ moves to position } j. \tag{6}$$

The permutation matrix is orthogonal, that is:

$$\boldsymbol{P}^{-1} = \boldsymbol{P}^T, \boldsymbol{P}^T \cdot \boldsymbol{P} = \boldsymbol{P} \cdot \boldsymbol{P}^T = \boldsymbol{1}_{2N} \tag{7}$$

where apex *T* denotes matrix transposition. Therefore, if $\boldsymbol{X}$ denotes the voltage or current vector of the reference bundle section, the voltage or current vector $\boldsymbol{X}'$ of the section obtained after the application of a cycle is

$$\boldsymbol{X}' = \boldsymbol{P} \cdot \boldsymbol{X}. \tag{8}$$

By such a linear transformation, one can easily prove that the MTL model of the *k*th bundle section (subscript *k*), accounting for the *k*th cycle applied to the preceding (subscript *k-1*) bundle section, is still formally similar to the MTL model in Fig. 6(a), where the chain-parameter matrix is recursively evaluated as

$$\boldsymbol{\Phi}_k = \begin{bmatrix} \boldsymbol{P}_k & \boldsymbol{0}_{2N} \\ \boldsymbol{0}_{2N} & \boldsymbol{P}_k \end{bmatrix} \cdot \boldsymbol{\Phi}_{k-1} \cdot \begin{bmatrix} \boldsymbol{P}_k^T & \boldsymbol{0}_{2N} \\ \boldsymbol{0}_{2N} & \boldsymbol{P}_k^T \end{bmatrix} \tag{9}$$

where $k = 1, 2, \ldots, N_S$, and the starting matrix $\boldsymbol{\Phi}_0$ pertains to the reference section, whereas voltage sources are obtained as

$$\boldsymbol{V}_{{\rm SL},k} = \left(\prod_{i=1}^{k} \boldsymbol{P}_{k+1-i}\right) \cdot \boldsymbol{V}_{\rm SL}, \quad \boldsymbol{V}_{{\rm SR},k} = \left(\prod_{i=1}^{k} \boldsymbol{P}_{k+1-i}\right) \cdot \boldsymbol{V}_{\rm SR}. \tag{10}$$

where $k = 1, 2, \ldots, N_S$, $\boldsymbol{0}_{2N}$ denotes the $2N \times 2N$null matrix. It is worth noting that the reference sources $\boldsymbol{V}_{\rm SL}$, $\boldsymbol{V}_{\rm SR}$ in the right sides of (10) depend on the incident electric field in the region of space occupied by the *k*th bundle section, and are evaluated only once, regardless of permutations, according to Section IV-A.

C. Prediction of the Terminal Response

For prediction of the terminal response, the MTL models of each bundle section are cascaded and the obtained chain-parameter representation—formally identical to the one in Fig. 6(a)—is then combined with the port constraints enforced by the terminal loads to determine the current, $\boldsymbol{I}_{\rm L}$, $\boldsymbol{I}_{\rm R}$ and voltage $\boldsymbol{V}_{\rm L}$, $\boldsymbol{V}_{\rm R}$ vectors (2*N* elements each) at the bundle terminals [16]. The process is schematically shown in Fig. 6(b). Without loss of generality, the terminal loads at the left (L) and right

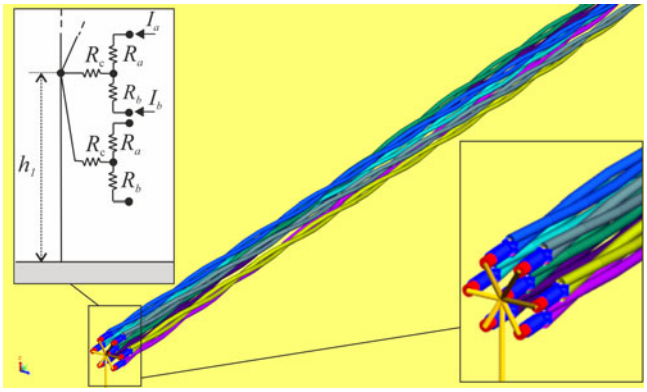

Fig. 7. Details of the implementation of the TWP bundle #1 (twined bundle) in a 3-D full-wave MoM solver, to obtain a reference solution used to validate the proposed MTL model.

(R) termination of the bundle are defined by $2N\times 2N$ impedance matrices (i.e., matrices $\boldsymbol{Z}_{\rm L}$, $\boldsymbol{Z}_{\rm R}$, respectively) with frequency-dependent entries.

V. Model Validation

To assess the validity of the approximations involved in treating a nonuniform MTL as the cascade of uniform MTLs with averaged p.u.l. parameters, the predictions obtained by the proposed model are here compared versus those obtained by full-wave (MoM-based) simulations. Such a validation leaves statistics out of consideration and is performed for two deterministic bundle configurations characterized by high nonuniformity.

Specifically, the bundle under analysis is characterized by the following data: $N = 7$, $r_w = 0.15$ mm, $s = 0.7$ mm, $s_b = 2$ mm, $h = h_1 = 5$ cm. Each TWP contains 40 twists having pitch 2.5 cm; therefore, the bundle length is 1 m. For every TWP in the bundle, terminal loads at both ends have a balanced T-configuration involving resistors $R_a = R_b = 50\,\Omega$, and $R_c = 100\,\Omega$, as shown in Fig. 7. The bundle is subdivided in $N_S = 10$ sections with length $\mathscr{L} = 10$ cm.

The following two sets of cycles are considered: 1) all the ten cycles are as in Fig. 3(b), leading to a *twined* TWP bundle (referred to as bundle #1 in the following); 2) all the ten cycles are as in Fig. 3(f), leading to a similar bundle, but where the central TWP does not move (bundle #2). These bundles were represented in a 3-D computer-aided design tool (spline curves were used to model TWP paths imposed by cycles [4], [11]), then imported and meshed with about 4000 wire segments in a MoM solver [20]. A detail of the left termination is shown in Fig. 7 for bundle #1. Circuit representations of such terminal sections (i.e., the so-called vertical risers) were included in the proposed model [7], [9].

As a specific choice for model validation, the impinging electromagnetic field is a uniform plane-wave characterized by electric-field strength $E_0 = 1$ V/m, incidence angles $\vartheta = 50°, \psi = 20°$, and polarization angle $\eta = 60°$ (see Fig. 8). For such a canonical excitation, the incident electric field along the bundle was computed by resorting to exact analytical expressions [7]. As a consequence, the discrepancies possibly observed in the presented validation can be only ascribed to approximation involved in the proposed MTL modeling approach.

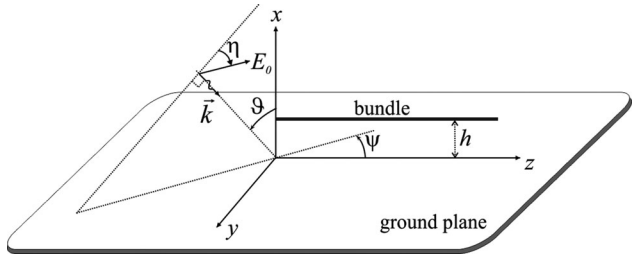

Fig. 8. Parameters of the plane-wave field.

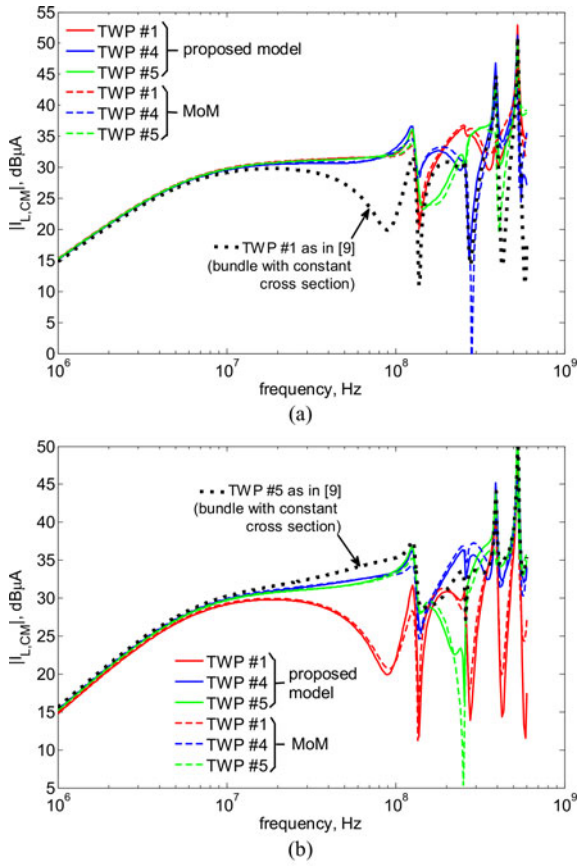

Fig. 9. CM currents induced in terminal loads of TWPs #1, #4 and #5. Proposed model (solid line) versus MoM simulation (dashed line): (a) bundle #1 (twined bundle); (b) bundle #2 (twined bundle with fixed central TWP #1).

Predictions obtained by the proposed model are compared versus MoM simulations in Fig. 9. The plotted quantity is the CM current in the left termination of a TWP (whose number is specified in the plot legend), defined as $I_{\rm L,CM} = I_a + I_b$ where I_a,I_b are the pair currents shown in Fig. 7. In particular, Fig. 9(a) refers to bundle #1, whereas Fig. 9(b) refers to bundle #2. The frequency range extends up to the empirical maximum frequency of validity of MTL modeling (such that $h_1 < \lambda/10$ where λ is the wavelength). Predictions are in good agreement with MoM solutions. Additionally, dotted black lines

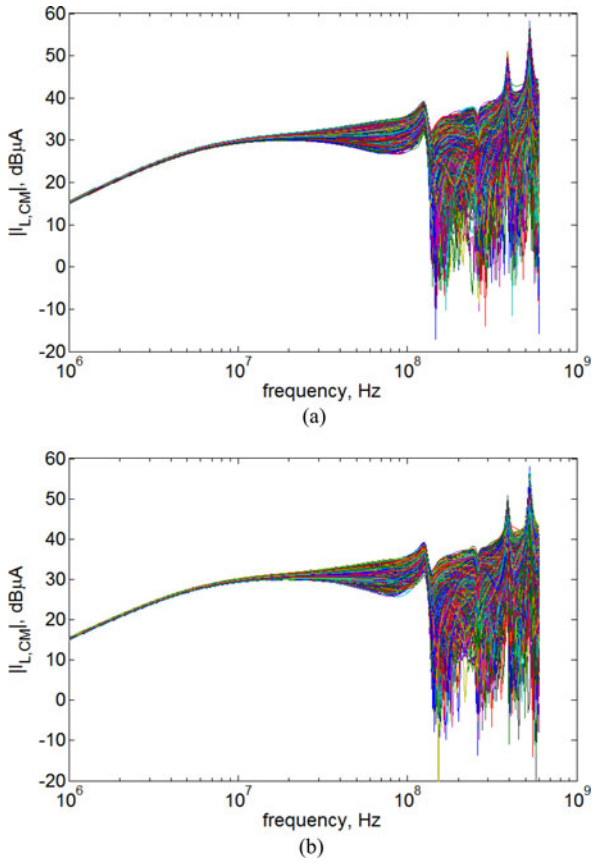

Fig. 10. CM currents induced in the left load of a TWP in the random bundle (10^4 samples): (a) TWP #1, (b) TWP #4.

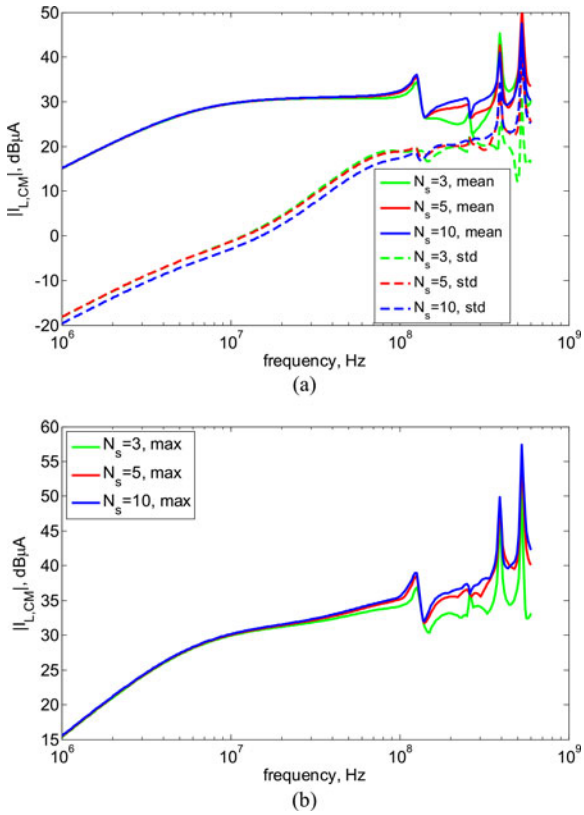

Fig. 11. Statistical estimates of the CM current induced in the left load of TWP #1 for different number N_S of bundle sections but equal bundle length (a) mean value: solid lines, standard deviation: dashed lines; (b) maximum.

in Fig. 9(a)–(b) represent results for specific TWPs in a bundle with constant cross section as in [9]. One can appreciate the difference between results of model [9] and the exemplified bundles, which confirms the need for proper modeling the variation of the cross section.

It is worth noting that the frequency response of the induced currents, when the bundle is electrically long, exhibits high sensitivity to bundle configurations. Indeed, one can appreciate substantial differences between Fig. 9(a) and (b) for all TWPs, although such figures refer to very similar bundles. Particularly, note that TWP #1 of bundle #2 [see Fig. 9(b)], which lies in a straight central position in the middle of the cross section, is subject to lower noise level than TWP #1 of bundle #1 [see Fig. 9(a)], which moves in all positions along the twined bundle. Such a noise reduction can be explained by the shielding effect that the external TWPs play on the internal ones [see Fig. 9].

In general, sensitivity to bundle configurations supports the need for the proposed MTL model, whose computational efficiency allows performing repeated-run simulations aimed at predicting, in a reasonable time, statistical estimates of noise currents induced in several samples of random bundles. Indeed, while the MoM solution (500 frequency points) for a single bundle in Fig. 9 required more than four hours of run-time on a six-core CPU (Intel i7 3.33 GHz) equipped with 24-GB RAM, the same results were obtained in about 1 s via the proposed model implemented in MATLAB.

VI. Statistical Analysis

A random TWP bundle illuminated by a plane-wave field with the same parameters defined in Section V is considered. By exploiting the procedure described in Section III, 10^4 bundle samples have been generated and modeled to compute the currents induced in terminal loads. The frequency response of CM currents induced in the left terminations of TWP #1 and #4 are plotted in Fig. 10(a) and (b), respectively.

Interesting observations follow from Fig. 10. Namely, in the low-frequency range, where the MTL is electrically short, the induced currents increase linearly with 20 dB/decade slope, and their sensitivity to different bundle configurations is practically negligible. Conversely, in the region of resonances, all curves spread out and fill the plot. In this case, the sensitivity to random bundle configurations is very high, since the induced current varies between a worst case, obtained as the envelope of all curves, and a minimum which is practically zero (notches of the frequency responses can be found almost at all frequencies).

Additionally, one can note that Fig. 10(a) and (b) are very similar. Therefore, even though for a specific bundle configuration the frequency response of the induced CM current may significantly differ from a TWP to another (as shown in Section V), the population of all frequency responses corresponding to different random configurations of the bundle is

practically the same for all TWPs. This is a consequence of the randomization of TWP positions in the bundle and of equal TWP loads.

Statistical estimates of the frequency response are reported in Fig. 11(a)–(b) for TWP #1 (computed in Ampere units and then plotted in dBμA units). Particularly, Fig. 11(a) is a plot of the mean value (solid lines) and standard deviation (dashed lines), whereas Fig. 11(b) shows the maximum. Additionally, Fig. 11(a)–(b) reports not only result for $N_{\rm S} = 10$ (i.e., the same case considered in Fig. 10), but also for lower numbers of bundle sections keeping unchanged the total bundle length of 1 m, that is, for $N_S = 3$ ($\mathscr{L} = 33.3$ cm) and $N_S = 5$ ($\mathscr{L} = 20$ cm). It is worth noting that the mean value, the standard deviation, and the maximum in Fig. 11(a)–(b) significantly depend on $N_{\rm S}$ in the high-frequency range. Moreover, one can show that the variation becomes negligible over a sufficiently large $N_{\rm S}$, to be correlated with the number *N* of TWPs. For the test-case here considered ($N = 7$), statistical estimates substantially reach convergence for $N_S \geq 10$. This is a significant indication that the statistics of the induced noise tends to a well-defined asymptotic behavior with an increasing number of bundle sections (that is, tending to a sort of *perfectly randomized* bundle).

VII. Conclusion

The approximate MTL model of field coupling to random TWP bundles was validated versus MoM and proved to be computationally efficient. Particularly, the proposed method allowed to 1) model the nonuniform TWP bundle as the cascade of uniform MTL sections; 2) generate random cross-sections ensuring minimum-distance shifts of TWPs; 3) derive the MTL model of each bundle section from a single MTL model through matrix permutations. The proposed model can handle coupling with nonuniform fields by following the approach in [9] for the numerical approximation of noise sources (4)–(5).

As a specific field structure of interest, a uniform plane-wave was considered, and the statistics of the induced CM noise was investigated. The statistical analysis (based on processing repeated-run simulations) pointed out that 1) noise sensitivity is significant for electrically long bundles, and 2) the statistics of noise does not depend on the considered TWP in the bundle, and converges to a unique solution for an increasing number of random-bundle sections.

The proposed method is limited to the prediction of CM noise in each pair of the bundle, and to that part of DM noise resulting from CM-to-DM conversion due to termination imbalance [9]. However, these noise components are of main interest for EMC purposes as they often represent dominant effects in the radiated-immunity phenomenon [13]. Model extension to the exact prediction of DM noise would require to account for twisting features here neglected, such as the effect of a noninteger number of twists [7] and twist nonuniformity [8]. Furthermore, a significant activity for future works will be the experimental validation of the statistical model through a measurement campaign performed in test chambers [21], [22].

References

[1] C. Jullien, P. Besnier, M. Dunand, and I. Junqua, "Crosstalk analysis in complex aeronautical bundle," in *Proc. EMC Europe*, Brugge, Belgium, Sept. 2–6, 2013, pp. 253–258.

[2] M. Wu, D. G. Beetner, T. H. Hubing, H. Ke, and S. Sun, "Statistical prediction of "reasonable worst-case" crosstalk in cable bundles," *IEEE Trans. Electromagn. Compat.*, vol. 51, no. 3, pp. 842–851, Aug. 2009.

[3] F. Paladian, P. Bonnet, and S. Lallechere, "Modeling complex systems for EMC applications by considering uncertainties," *in Proc. 30th URSI General Assembly Sci. Symp.*, Istanbul, Turkey, Aug. 13–20, 2011, pp. 1–4.

[4] S. Sun, G. Liu, J. L. Drewniak, and D. J. Pommerenke, "Hand-assembled cable bundle modeling for crosstalk and common-mode radiation prediction," *IEEE Trans. Electromagn. Compat.*, vol. 49, no. 3, pp. 708–718, Aug. 2007.

[5] C. Jullien, P. Besnier, M. Dunand, and I. Junqua, "Advanced modeling of crosstalk between an unshielded twisted pair cable and an unshielded wire above a ground plane," *IEEE Trans. Electromagn. Compat.*, vol. 55, no. 1, pp. 183–194, Feb. 2013.

[6] A. Shoory, M. Rubinstein, A. Rubinstein, C. Romero, N. Mora, and F. Rachidi, "Application of the cascaded transmission line theory of Paul and McKnight to the evaluation of NEXT and FEXT in twisted wire pair bundles," *IEEE Trans. Electromagn. Compat.*, vol. 55, no. 4, pp. 648–656, Aug. 2013.

[7] S. A. Pignari and G. Spadacini, "Plane-wave coupling to a twisted-wire pair above ground," *IEEE Trans. Electromagn. Compat.*, vol. 53, no. 2, pp. 508–523, May 2011.

[8] G. Spadacini and S. A. Pignari, "Numerical assessment of radiated susceptibility of twisted-wire pairs with random nonuniform twisting," *IEEE Trans. Electromagn. Compat.*, vol. 55, no. 5, pp. 956–964, Oct. 2013.

[9] G. Spadacini, F. Grassi, F. Marliani, and S. A. Pignari, "Transmission-line model for field-to-wire coupling in bundles of twisted-wire pairs above ground," *IEEE Trans. on Electromagn. Compat.*, vol. 56, no. 6, pp. 1682–1690, Dec. 2014.

[10] M. Magdowski and R. Vick, "Simulation of the stochastic electromagnetic field coupling to an unshielded twisted pair of wires," in *Proc. IEEE Int. Symp. on Electromagn. Compat.*, Denver, CO, USA, Aug. 5–9, 2013, pp. 33–37.

[11] D. Bellan and S. Pignari, "Efficient estimation of crosstalk statistics in random wire bundles with lacing chords," *IEEE Trans. Electromagn. Compat.*, vol. 53, no. 1, pp. 209–218, Feb. 2011.

[12] M. Omid, Y. Kami, and M. Hayakawa, "Field coupling to uniform and nonuniform transmission lines," *IEEE Trans. Electromagn. Compat.*, vol. 39, no. 3, pp. 201–211, Aug. 1997.

[13] F. Grassi, G. Spadacini, and S. A. Pignari, "The concept of weak imbalance and its role in the emissions and immunity of differential lines," *IEEE Trans. Electromagn. Compat.*, vol. 55, no. 6, pp. 1346–1349, Dec. 2013.

[14] G. H. Danielson, "On finding the simple paths and circuits in a graph," *IEEE Trans. Circuit Theory*, vol. 15, no. 3, pp. 294–295, Sept. 1968.

[15] G. Spadacini, D. Bellan, and S. Pignari, "Impact of twist non-uniformity on crosstalk in twisted-wire pairs", in *Proc. IEEE Symp. On Electromagn. Compat.* Boston, MA, USA, Aug. 18–22, 2003, pp. 483–488.

[16] C. Paul, *Analysis of Multiconductor Transmission Lines*. New York, NY: Wiley-Interscience, 1994.

[17] A. K. Agrawal, H. J. Price, and S. H. Gurbaxani, "Transient response of multiconductor transmission-lines excited by a nonuniform electromagnetic field," *IEEE Trans. Electromagn. Compat.*, vol. EMC-22, no. 2, pp. 119–129, May 1980.

[18] M. Leone and H. L. Singer, "On the coupling of an external electromagnetic field to a printed circuit board trace," *IEEE Trans. Electromagn. Compat.*, vol. 41, no. 4, pp. 418–424, Nov. 1999.

[19] G. Spadacini, S. A. Pignari, and F. Marliani, "Closed-form transmission line model for radiated susceptibility in metallic enclosures," *IEEE Trans. Electromagn. Compat.*, vol. 47, no. 4, pp. 701–708, Nov. 2005.

[20] FEKO Suite 6.3 User's Manual (Oct. 2013), © EM Software and Systems, S.A.(Pty) Ltd, Stellenbosch, South Africa, www.feko.info

[21] G. Spadacini, S. A. Pignari, and F. Marliani, "Experimental measurement of the response of a twisted-wire pair exposed to a plane-wave field," in *Proc. IEEE Int. Symp. Electromagn. Compat.*, Long Beach, CA, USA, 2011, pp. 828–833.

[22] M. Magdowski, J. Ladbury, C. Holloway, and R. Vick, "Measurement of the stochastic electromagnetic field coupling to an unshielded twisted pair cable," in *Proc. Int. Symp. Electromagnetic Compatibility (EMC Europe)*, Gothenburg, Sweden, Sept. 1–4, 2014, pp. 659–664.